

L. ANGKURARACH\*, P. JUIJERM\*

## EFFECTS OF DIRECT CURRENT FIELD ON POWDER-PACKED BORIDING PROCESS ON MARTENSITIC STAINLESS STEEL AISI 420

### WPLYW POLA PRĄDU STAŁEGO NA UTWARDZANIE DYFUZYJNE BOREM POWIERZCHNI MARTENZYTYCZNEJ STALI NIERDZEWNEJ AISI 420

The effects of direct current field on a powder-packed boriding process on a martensitic stainless steel AISI 420 have been investigated at a temperature of 900 °C for about 2–6 hr. A powder-packed boriding process without direct current field (conventional powder-packed boriding process, PB) is a reference as compared to the powder-packed boriding process with applied current densities (PB-DC) of 60-170 mA/cm<sup>2</sup>. The microstructure and the presence of boride layers of PB and PB-DC were characterized using optical microscope and X-ray diffraction (XRD). The hardness values of the boride layer were measured by Vickers microhardness tester. Experimental results show that the direct current field can enhance the decomposition and chemical reaction in the boriding agent and also drive active free boron ions as well as atoms to diffuse toward the cathode. Therefore, a boron concentration around the specimen at the cathode of PB-DC is higher than that at the anode as well as PB (as a reference). As a consequence, higher boride layer thickness of PB-DC was detected. The double-phase boride layer (FeB and Fe<sub>2</sub>B) on borided martensitic stainless steel AISI 420 was found both PB and PB-DC. The hardness of the boride layer of about 1800–2000 HV can be observed.

*Keywords:* Thermochemical surface treatment; Boriding process; Stainless steel; Direct current field

Badano wpływ pola prądu stałego proces utwardzania borem martenzytycznej stali nierdzewnej AISI 420 w temperaturze 900°C przez około 2 do 6 godzin. Konwencjonalny proces borowania (bez prądu stałego, PB) jako proces referencyjny porównano z procesem borowania z zastosowaniem gęstości prądu 60-170 mA/cm<sup>2</sup> (PB-DC). Mikrostruktura i obecność warstw borków w przypadku procesów PB i PB-DC scharakteryzowano za pomocą mikroskopu optycznego i dyfrakcji rentgenowskiej (XRD). Twardości warstw borków były mierzone przez pomiar mikrotwardości Vickersa. Wyniki eksperymentu wskazują, że pole prądu stałego może zwiększyć rozkład i reakcję chemiczną w czynniku borującym, a także ukierunkować dyfuzję aktywnych wolnych jonów boru jak również atomów w kierunku katody. Dlatego stężenie boru wokół próbki na katodzie w procesie PB-DC jest wyższe niż na anodzie, jak i wyższe niż w procesie PB (jako punkt odniesienia). W rezultacie grubość warstwy borków jest większa w procesie PB-DC. Dwu-fazowe warstwy borków (FeB i Fe<sub>2</sub>B) na utwardzanej powierzchniowo-martenzytycznej stali nierdzewnej AISI 420 stwierdzono w przypadku procesów PB i PB-DC. Twardość warstwy borków wynosi ok. 1800-2000 HV.

## 1. Introduction

Stainless steels are widely used in the engineering and medical field because they are the iron-base alloys given to a group of corrosion resistance steel. However, complicated and high-load applications are much more required in the present and the future, especially for steels having a martensitic structure such as a martensitic stainless steel AISI 420. Applications of martensitic stainless steels are such as structural parts, industrial tooling, cutlery, mold and others. Therefore, problems about wear resistance on the martensitic stainless

steels increase considerably. Surface modification to improve wear resistance for the martensitic stainless steel is therefore mentioned frequently. Boriding is a one of well-known thermochemical surface hardening process which possesses a high surface hardness, good wear resistance, heat resistance, corrosion and oxidation resistance [1,2]. The PB is carried out usually at the temperature range of 850–1000 °C for about 3–8 hr to obtain a boride layer (FeB and Fe<sub>2</sub>B). Active boron ions as well as atoms are generated from thermal decomposition of certain constituent in the powder agent and chemical reaction between constituents of the agent at a high tem-

\* DEPARTMENT OF MATERIALS ENGINEERING AND CENTER OF ADVANCED STUDIES IN INDUSTRIAL TECHNOLOGY, FACULTY OF ENGINEERING, KASETSART UNIVERSITY, 50 NGAMWONGWAN RD., LADYAO, JATUJAK, BANGKOK 10900, THAILAND

perature. Active boron ions as well as atoms are diffused into metal surfaces in order to enhance the surface properties and formed the boride layer. Boriding process involves a diffusion controlled coating. Thus, the thickness of boride layer depends strongly on the chemical composition of the substrate, boron potential of boriding composition, temperature and soaking time of boriding process [1-3]. Generally, the boriding processes are carried out at a high temperature with long soaking time as a consequence of much energy consuming and high operating cost. A basic concept to solve the problems is to increase the diffusion rate of boron atoms. So, important factors such as boron potential, boriding temperature and boriding time are considered taking into account the Fick's laws [4,5]. Nevertheless, increasing boriding temperature and soaking time causes certainly high energy consuming. Many industries are not appreciated certainly for that way. Thus, the boron potential is an alternative way to increase the diffusion rate of boron atoms. The greater boron potential should increase the diffusion rate taking into account the diffusion theory. It shall be expected if the decomposition and chemical reactions in the boriding agent are improved and then the active boron atoms can be forced also to move mainly and directionally to the specimen's surface. Electric field is a method which can supply an extra energy to the agent and promote the decomposition and chemical reactions and also determine the moving direction of ions [6,7]. Therefore, direct current field should possibly determine the moving direction of active boron ions as well as atoms in the boriding processes and increase the boron potential of the powder-packed boriding process. For these reasons, the effects of direct current field on a powder-packed boriding process on a martensitic stainless steel AISI 420 will be investigated and addressed. The PB is a reference as compared to the PB-DC with current densities of 60-170 mA/cm<sup>2</sup> at a temperature of 900°C for 2–6 hr. Microstructures, thickness and hardness depth profiles are investigated and shown in this research.

## 2. Material and methods

The martensitic stainless steel AISI 420 was delivered as hardened and tempered bars with a diameter of 12.5 mm. The chemical composition of this alloy is 0.3%

C, 0.25% Si, 0.43% Mn, 0.018% P, 0.028% S, 0.32% Ni, 12.15% Cr and Fe balance (all values in wt.%). Cylindrical specimens with a diameter of 12.5 mm and a height of 20 mm were prepared from bars of the martensitic stainless steel AISI 420. All samples were ground with 600 grit SiC paper to clean the surface. The boriding powder used in this experiment was commercial boriding agent named Ekabor-I from BorTec GmbH, Germany. In the boriding process, samples for the reference, cathode and anode were placed with a distance of 15 mm and packed as well as buried in Ekabor-I powder into a steel container with a lid and cement seal. The steel container was heated using an electrical furnace with argon atmosphere. Boriding process was performed at a temperature of 900°C duration 2–6 hr. The current densities in the range of 60–170 mA/cm<sup>2</sup> were applied between the two electrodes (cathode and anode samples) during boriding process for PB–DC. The temperature of reference as well as electrodes was measured with a thermocouple type K by drilling a hole in the samples. Microstructures and kind of the existing layers were characterized using an optical microscope and X-ray diffraction (XRD) with Cu K $\alpha$  radiation source ( $\lambda = 0.154$  nm), respectively. The thicknesses were measured using the optical microscope with an image analyzer program. The hardness depth profiles were measured using the Vicker microhardness tester with a load of 50 g.

## 3. Results

### 3.1. Powder-packed boriding process without direct current field, PB (as a reference)

After PB at a temperature of 900°C duration about 2, 4 and 6 hr, boride layers were formed on the martensitic stainless steel AISI 420 as depicted in Fig. 1 illustrating the boride layer formed at a temperature of 900°C for about 4 hr as an example. The formed boride layers on the martensitic stainless steel AISI 420 have smooth and more compact morphology as compared to low or unalloyed steels [1,2]. The presence of boride layer is double-phase (FeB and Fe<sub>2</sub>B), which FeB phase is at the surface and near surface regions and Fe<sub>2</sub>B phase is beneath and connected to the substrate. It can be confirmed this double phase boride layer by the XRD spectrums

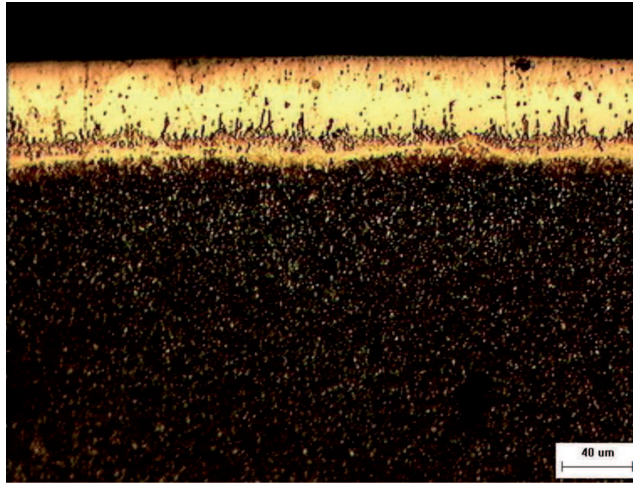


Fig. 1. The cross-sectional boride layer of the PB at a temperature of 900°C for about 4 hr

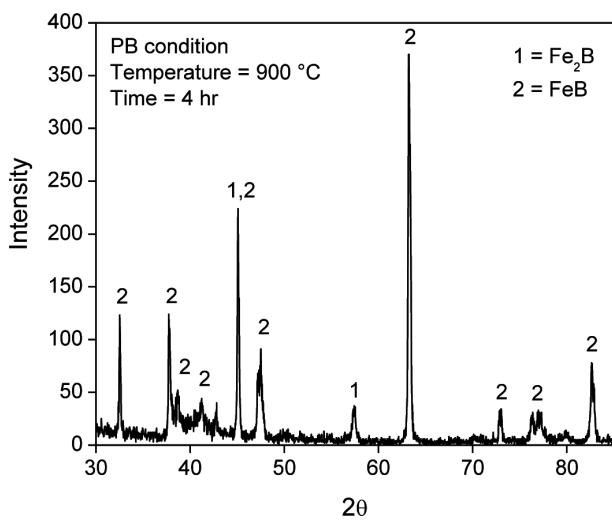


Fig. 2. X-ray diffraction patterns of the PB at a temperature of 900°C for about 4 hr

as shown in Fig. 2 which illustrates the XRD patterns of the martensitic stainless steel AISI 420 borided at a temperature of 900°C for about 4 hr. Moreover, the thickness of the boride layer increases with increasing boriding time following the diffusion theory. The change in boride layer thickness with boriding time is given in Fig. 3a. Assuming that progress of boride layer obeys parabolic law, the squared thickness of boride layer as a function of time can be described as follows [3-5,10-13]:

$$d^2 = Kt \quad (1)$$

where  $d$  is depth of boride layer (m),  $t$  is process time (s),  $K$  is the growth rate constant depending on the boriding temperature and can be determined by a slope of a straight line in a diagram of  $d^2$  as a function of boriding time at a given boriding temperature as shown in Fig. 3b. The measured data are fitted by straight lines with a slope of approximately  $K_{PB} = 1.13 \times 10^{-13} \text{ m}^2/\text{s}$  for the PB at a boriding temperature of 900 °C with various boriding times. The near surface hardness of boride

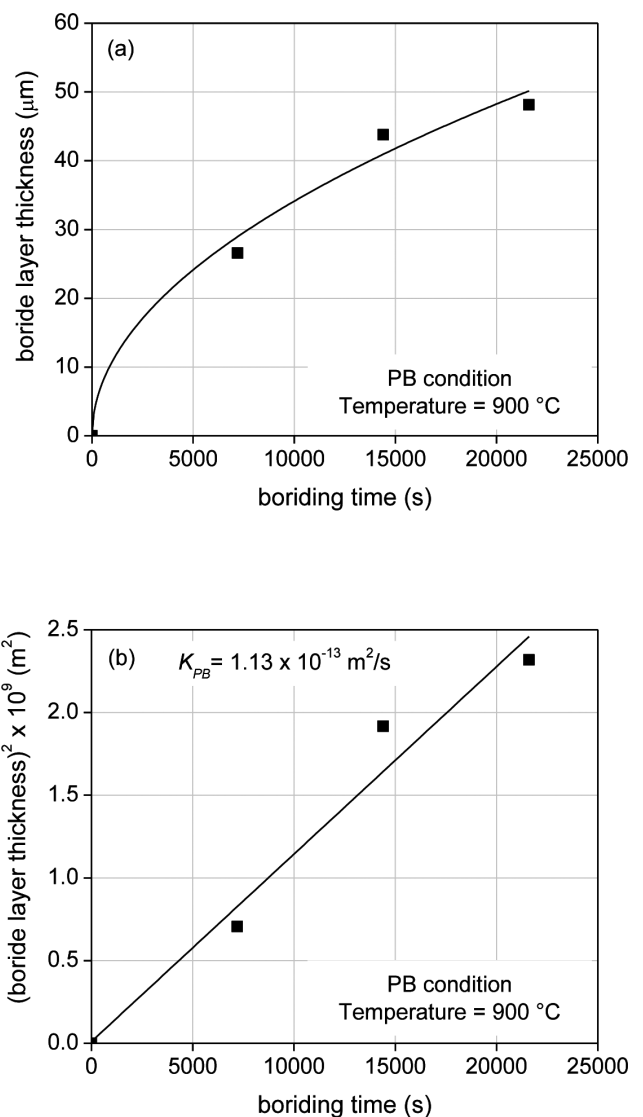


Fig. 3. The diagrams of (a) the boride layer thickness values and (b) square of the boride layer thickness values of the PB versus boriding time

layer could be reached about more than 1800 HV, whereas the hardness values of the substrate of only approximately 500 HV were measured. The hardness depth profile of the martensitic stainless steel AISI 420 borided at a temperature of 900°C for about 4 hr was measured as shown in Fig. 4.

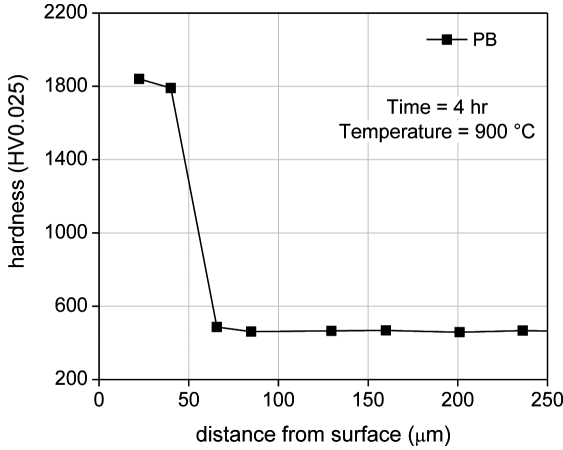


Fig. 4. Hardness depth profile of the PB at a temperature of 900°C for about 4 hr

### 3.2. Powder-packed boriding process with direct current field, PB-DC

Firstly, to clarify the effects of the direct current on the powder-packed boriding process, various current densities of 0, 60, 120 and 170 mA/cm<sup>2</sup> was applied to the powder-packed boriding process at a constant boriding temperature of 900°C for about 4 hr. Fig. 5 depicts the boride layer thickness versus the current densities. It was found that the current density of 120 mA/cm<sup>2</sup> or higher can enhance the diffusion rate of boron atoms in the powder-packed boriding process. Thickest value of 75 μm was detected at an applied current density of 170 mA/cm<sup>2</sup> after powder-packed boriding process at a temperature of 900°C for about 4 hr, whereas the thickness of the PB at the same condition of only about 48 μm was measured (about 56.25 % increment of boride layer thickness). Temperatures at the cathode and anode were also measured during applying current density as shown in Fig. 6. It indicated that the real temperature of samples at electrodes (cathode and anode) increases when the direct current increases. The maximum temperature of about 930°C was detected at electrodes, when the current density of 170 mA/cm<sup>2</sup> was applied. An increase of temperature at the cathode affects more or less the diffusion rate of active boron atoms in a positive way. The PB-DC with current density of 170 mA/cm<sup>2</sup> was investigated further for different boriding times of 2, 4 and 6 hr. The exemplary microstructures of the boride layers after the PB-DC as compared to the PB at the same process parameters are shown in Figs. 7a-b illustrating the near surface microstructures of PB and PB-DC at a temperature of 900°C for about 6 hr. The greater boride layer of the PB-DC was observed clearly. However, characteristics of boride layers of the PB-DC are so related

to of the PB. That means that the formed boride layers after PB-DC have also smooth and compact morphology. Double phases, FeB and Fe<sub>2</sub>B are mainly observed through microstructures (see Fig. 7a). The boride layer thicknesses of PB-DC increase with increasing boriding time as shown in Fig. 8a and also obey parabolic law in Eq. 1. The growth rate constant,  $K_{PB-DC}$  can be determined by a slope of a straight line in a diagram of  $d^2$  as a function of boriding time at a constant boriding temperature as shown in Fig. 8b. The measured data are fitted by straight lines with a slope of approximately  $K_{PB-DC} = 3.09 \times 10^{-13} \text{ m}^2/\text{s}$  for the PB-DC at a boriding temperature of 900°C with various boriding times. It can be seen that at the boriding temperature of 900°C the growth rate of the powder-packed boriding with applied direct current,  $K_{PB-DC}$  is higher than the growth rate of the powder-packed boriding without applied direct current,  $K_{PB}$ . It can be mentioned that the boride layer formed by the PB-DC should be thicker than that formed by the PB at a boriding temperature of 900°C for the same soaking time. The near surface hardness of boride layer of approximately 2000 HV was measured after the PB-DC at a temperature of 900°C for about 4 hr and then decreased to the substrate (approximately 500 HV) as shown in Fig. 9.

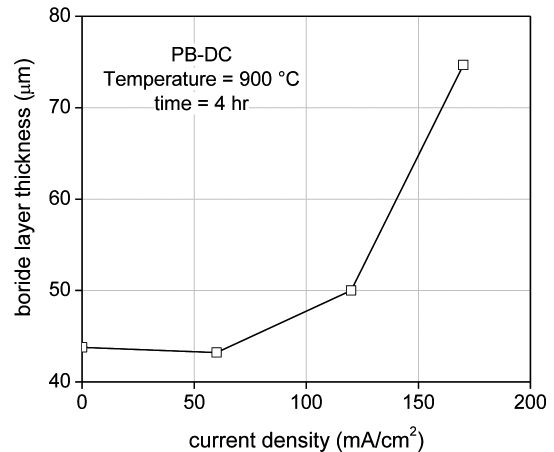


Fig. 5. Boride layer thickness values of the PB-DC versus current densities

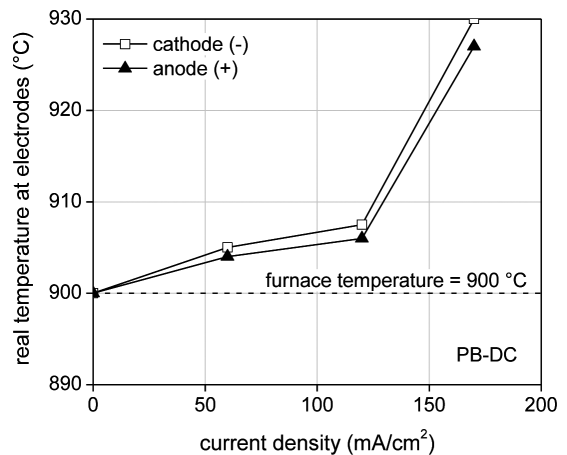


Fig. 6. The real temperatures at electrodes of the PB-DC for different current densities

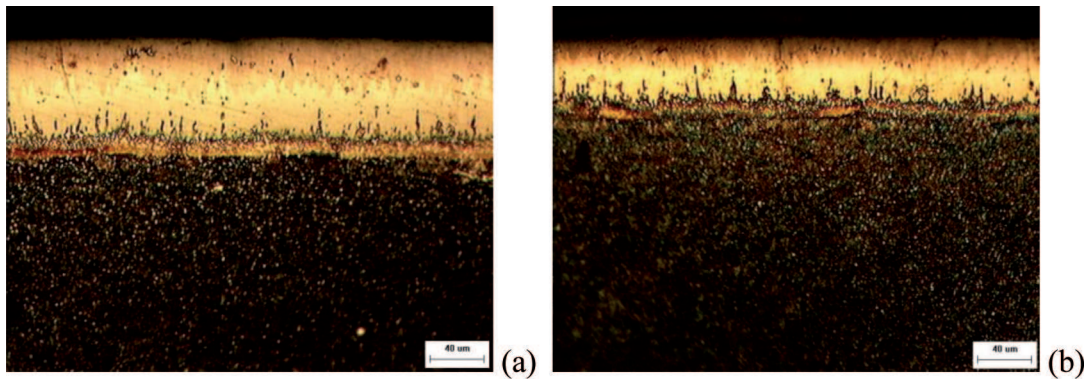


Fig. 7. The cross-sectional boride layers of the (a) PB-DC and (b) PB at a temperature of 900°C for about 6 hr

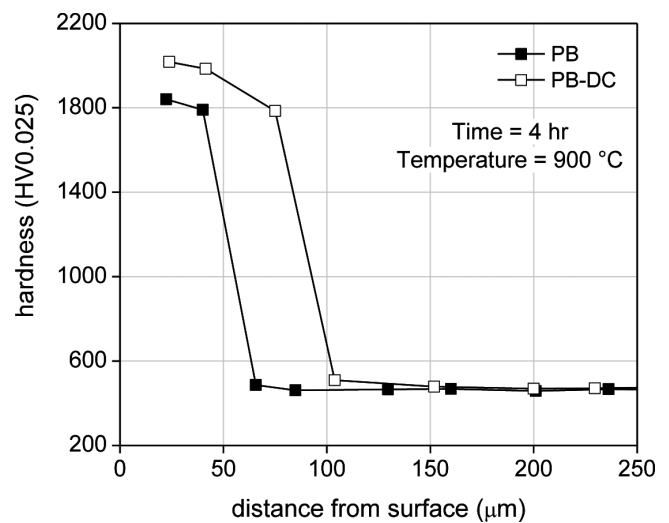
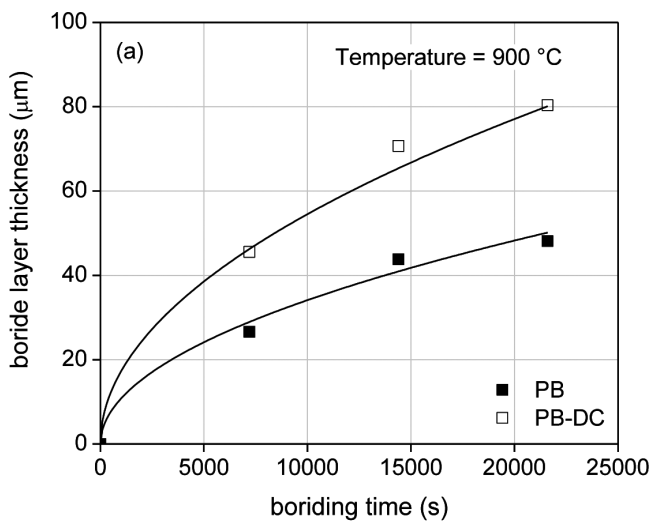


Fig. 9. Hardness depth profiles of the PB-DC and PB at a temperature of 900°C for about 4 hr

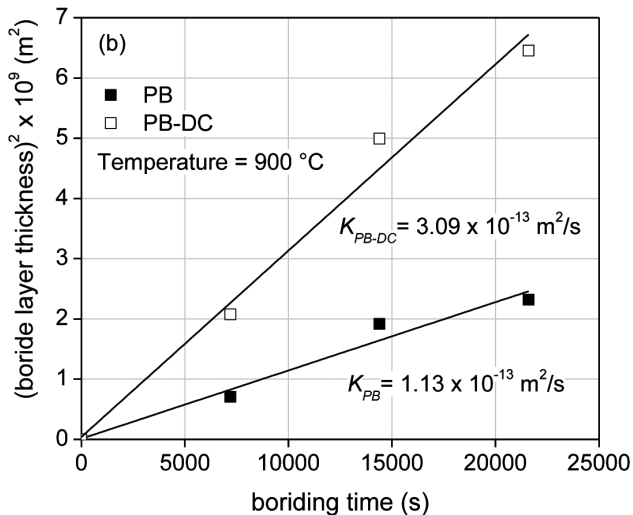


Fig. 8. The diagrams of (a) the boride layer thickness values and (b) square of the boride layer thickness values of the PB-DC and PB versus boriding time

#### 4. Discussion

The formed boride layers on the martensitic stainless steel AISI 420 have smooth and more compact morphology due to presenting of high alloying elements. The characteristic sawtooth configuration of the boride layer is dominant with unalloyed low carbon steels and low alloy steels. As the alloying element and/or carbon content of the substrate are increased, the development of a jagged boride/substrate interface is suppressed. Alloying elements in the martensitic stainless steel AISI 420 retard mainly the boride layer thickness caused by restricted diffusion of boron atoms into the steel [1,2,8,9]. Double phase, FeB and Fe<sub>2</sub>B was detected regularly and clearly. The outside dark color phase is FeB and then the Fe<sub>2</sub>B (bright color phase) beneath the FeB layer (see Figs. 1 and 7a-b). The XRD pattern in Fig. 2 can be used also a confirmation. From experimental results, the beneficial effects of the direct current field on the powder-packed boriding process were observed certain-

ly on the boride layer thickness in the Figs. 7a-b and 8a-b. The greater thickness values of the PB-DC were measured as compared to the PB at the same process parameters. That means that the diffusion rate of boron atoms was enhanced by the direct current fields. The effects of the direct current field could be divided into two categories, thermal and physical effects. The direct current field has thermal effects on the cathode and anode (see Fig. 6) which could activate the chemical reaction of the boron ions in diffusion into the surface and increased more or less the diffusion rate. For the physical effects, moreover, the direct current field supplies an extra energy to the boriding agent and promotes the decomposition and chemical reactions in the boriding agent, which can increase the activity and concentration of active boron ions. Additionally, when sufficient direct current and voltage was applied to anode and cathode, the boron ions (positive charge) should be forced to move directionally toward to cathode by the electrical field. It can be mentioned that a sufficient electrical field can determine the moving direction of active boron ions toward to the cathode's surface and therefore increase the boron potential around the cathode of the PB-DC. Consequently, the obvious direction of diffusion should be faster and better than the random by only thermal effect [6,14]. Some experimental results supporting above assumption are the higher thicknesses of FeB (the outer phase of the boride layer) after the PB-DC (see Fig. 7a) as compared to the thickness of FeB after the PB (see Fig. 7b). An occurring of the FeB phase at the outer of the treated specimen indicates that boriding process is operated with high boron potential, high boriding temperature or prolonged soaking time [1,2]. For the same conditions of the powder-packed boriding process parameters, e.g. temperature and soaking time, higher thickness of FeB phase should be caused by higher boron potential which was related to the effects of the direct current field of the PB-DC. Finally, it can be concluded that an applying direct current field is therefore a possible way to enhance the powder-packed boriding process

## 5. Conclusions

In this research, the effects of the direct current on the powder-packed boriding process have been investigated and clarified. The martensitic stainless steel AISI 420 was borided using PB at a temperature of 900°C for various boriding times and then compared to the PB-DC. The main results are summarized as follows:

1. An applying sufficient direct current field (current density of about 120 mA/cm<sup>2</sup> or above) is a possible

way to enhance the powder-packed boriding process due to thermal and physical effects lead to increase boron potential and an effective move as well as diffusion of boron ions (positive charge) toward to the cathode's surface.

2. An applied current density of 170 mA/cm<sup>2</sup> during the powder-packed boriding process can increase thickness of the boride layer more than 50% as compared to the conventional powder-packed boriding process at a temperature of 900°C for the same soaking time.
3. The boride layer formed on the martensitic stainless steel AISI 420 (both PB and PB-DC) revealed a smooth and compact morphology due to high alloying elements. Very high hardness values of the boride layer approximately 1800–2000 HV were observed.

## Acknowledgements

The authors would like to express sincere thanks to the Center of Advanced Studies in Industrial Technology and Graduate School of Kasetsart University, Thailand for financial support for Ms. L. Angkurarach. Thanks is also due to Ms. P. Chamchongkaset for some experimental works.

## REFERENCES

- [1] J.R. Davis, Surface hardening of steels: Understanding the Basics, ASM International, 213-226 (2002).
- [2] A.K. Sinha, In: ASM Handbook vol. 4. Heat treating, ASM International, 437-447 (1991).
- [3] S. Sen, U. Sen, C. Bindal, Surf Coat Tech. **191**, 274-285 (2005).
- [4] R.E. Reed-Hill, Physical metallurgy principles, third ed., PWS Publishing Company (1991).
- [5] P.G. Shewmon, Diffusion in solids, second ed., The Minerals, Metals & Materials Society (1989).
- [6] Z. Zhou, F. Xie, J. Hu, Surf Coat Tech. **203**, 23-27 (2008).
- [7] M. Schlesinger, M. Paunovic, Modern Electroplating, fourth ed., John Wiley & Sons, Inc. (2000).
- [8] I. Ozbek, S. Sen, M. Ipek, C. Bindal, S. Zeytin, A.H. Ucisik, Vacuum. **73**, 643-648 (2004).
- [9] I. Ozbek, B.A. Konduk, C. Bindal, A.H. Ucisik, Vacuum. **65**, 521-525 (2002).
- [10] K. Genel, Vacuum. **80**, 451-457 (2006).
- [11] S. Sen, U. Sen, C. Bindal, Vacuum. **77**, 195-202 (2005).
- [12] K. Genel, I. Ozbek, C. Bindal, Mater. Sci. Eng. **A 347**, 311-314 (2003).
- [13] O. Ozdemir, M.A. Omar, M. Usta, S. Zeytin, C. Bindal, A.H. Ucisik, Vacuum. **83**, 175-179 (2009).
- [14] F. Xie, Q.H. Zhu, J.J. Lu, Solid State Phenom. **118**, 167-171 (2006).